

Liquid-Vapor Interface in Liquid Binary Alloys: An *Ab Initio* Molecular Dynamics Study

D. J. González,¹ L. E. González,¹ and M. J. Stott²

¹*Departamento de Física Teórica, Facultad de Ciencias, Universidad de Valladolid, 47011 Valladolid, Spain*

²*Department of Physics, Queen's University, Kingston, Ontario, Canada K7L 3N6*

(Received 16 December 2004; published 23 February 2005)

We report the results of an *ab initio* molecular dynamics simulation of the liquid-vapor interface of two binary liquid alloys, $\text{Na}_{0.3}\text{K}_{0.7}$ and $\text{Li}_{0.4}\text{Na}_{0.6}$, whose bulk behavior exhibits rather differing ordering tendencies. The study has been performed using samples of 2000 and 3000 particles, respectively, in a slab geometry with periodic boundary conditions. In both cases, the total ionic density distributions along the normal to the interface display some layering with a virtually pure monolayer of the lower surface tension component located outermost at the interface. However, the two systems behave very differently below the interface which can be accounted for by their different ordering tendencies in the bulk.

DOI: 10.1103/PhysRevLett.94.077801

PACS numbers: 61.25.Mv, 64.70.Fx, 71.15.Pd

Research into the structure of the liquid-vapor interface has produced theoretical and experimental work [1]. Grazing incidence x-ray diffraction and x-ray reflectivity (XR) have been the main experimental techniques for studying the liquid-vapor interface. The application to several liquid metals (Hg, Ga, In, and K) [2] and alloys (Na-K, In-Ga, Bi-Ga, Bi-In, and Sn-Ga) [3–5] has concluded that the interface exhibits an oscillatory surface-normal (longitudinal) density profile which extends several atomic diameters into the bulk liquid. In contrast, XR measurements on different nonmetallic liquids [6] show a density profile with a smooth monotonic decay from the high density bulk liquid to the low density vapor.

The possibility of surface layering in liquid metals was raised by Rice and co-workers nearly three decades ago. The results of their Monte Carlo (MC) simulations for liquid metals [7,8] and binary alloys [5,9], using density dependent pair potentials, suggested that surface layering is due to the coupling between the ionic and electronic densities and that the abrupt decay of the electronic density profile induces an effective wall against which the ions, behaving like hard spheres, stack. Moreover, in the specific case of homovalent binary alloys, Rice and co-workers [5,9] found some common structural features of the interface: (i) the total ionic longitudinal density profile is stratified for 3-4 atomic diameters into the bulk liquid, (ii) the lower surface tension component segregates and forms a nearly pure surface monolayer, and (iii) there is a deficiency, relative to the bulk concentration, of that component in the second layer of the stratified interface with the bulk concentration reached at the fourth atomic layer. However, these conclusions were drawn from MC simulations on liquid binary alloys with weak ordering tendencies in the bulk [5,9] and could be modified for systems with strong homo-(segregating) or heterocoordinating (compound forming) tendencies. In fact, an XR measurement [3] of the liquid-vapor interface in $\text{Bi}_{0.22}\text{In}_{0.78}$, which has significant heterocoordinating tendencies, suggests that the outer layer has a Bi concentration of only ≈ 0.35 .

In this Letter, we present *ab initio* molecular dynamics (MD) calculations of the liquid-vapor interface in the liquid $\text{Na}_{0.3}\text{K}_{0.7}$ and $\text{Li}_{0.4}\text{Na}_{0.6}$ alloys. A great deal of theoretical [10,11] and experimental [12–15] work has already been devoted to the bulk structural and thermodynamic properties of these alloys. The $\text{Na}_{0.3}\text{K}_{0.7}$ shows mild homocoordinating tendencies, and recently, a XR study has been carried out on the surface structure of the liquid $\text{Na}_{0.33}\text{K}_{0.67}$ alloy [3] making this system worthy of investigation. The reflectivity measurements were limited to small wave vector transfers ($q_z \leq 1 \text{ \AA}^{-1}$, where q_z is the momentum transfer normal to the surface), well below the value for the position of the expected layering peak (i.e., $q_z \approx 1.7 \text{ \AA}^{-1}$); nevertheless, the associated surface structure factor $\phi(q_z)$ showed features indicating some surface layering. Even though no corresponding theoretical and/or experimental work has been carried out on the liquid-vapor interface of the liquid $\text{Li}_{0.4}\text{Na}_{0.6}$ alloy, we have also chosen this system because of its strong homocoordinating tendencies in the bulk [11].

This study has been performed using the orbital-free *ab initio* molecular dynamics (OF-AIMD) method, where the forces acting on the nuclei are computed from the electronic structure calculated within density functional theory (DFT) [16,17]. The interactions between atoms depend on the electronic structure. In a metallic system, the nature of the interactions changes drastically across the liquid-vapor interface, and therefore it is crucial that the forces on the atoms react to the electronic density distribution in their vicinity. This is achieved in the OF-AIMD method by using an explicit but approximate density functional for the electron kinetic energy. This leads to a substantial simplification over the commonly used Kohn-Sham method of DFT [17] which achieves greater accuracy but at the cost of much greater computational expense. The OF-AIMD makes possible the simulation of large samples for long times.

A liquid simple metal alloy, A_xB_{1-x} , can be regarded as an assembly of N_A , A -type, and N_B , B -type, bare ions with

charges Z_v^A and Z_v^B , respectively, enclosed in a volume Ω and interacting with $N_e = N_A Z_v^A + N_B Z_v^B$ valence electrons through electron-ion potentials $v_A(r)$ and $v_B(r)$. The total potential energy of the system can be written, within the Born-Oppenheimer approximation, as the sum of the direct ion-ion Coulombic interaction energy and the ground state energy of the electronic system, $E_g[\rho_g(\vec{r})]$. According to DFT, the ground state electronic density, $\rho_g(\vec{r})$, minimizes an energy functional which is the sum of the kinetic energy of independent electrons, $T_s[\rho]$, the classical Hartree electrostatic energy, $E_H[\rho]$, the exchange-correlation energy, $E_{xc}[\rho]$, for which we have adopted the local density approximation and the electron-ion interaction energy, $E_{ext}[\rho]$, for which we have used local ionic pseudopotentials constructed within DFT [18].

The functional $T_s[\rho]$ includes the von Weizsäcker term plus further terms chosen in order to reproduce correctly some exactly known limits [18]. The local ionic pseudopotentials were constructed from first principles by fitting the displaced electronic density induced by an ion immersed in a metallic medium as obtained in a Kohn-Sham calculation. Further details are given in Ref. [18], and we note that the theoretical framework used here has provided an accurate description of several static and dynamic properties of bulk liquid Li, Mg, Al, Na-Cs, and Li-Na systems [11,18,19].

OF-AIMD simulations have been performed for the liquid-vapor interfaces of the $\text{Na}_{0.3}\text{K}_{0.7}$ and $\text{Li}_{0.4}\text{Na}_{0.6}$ alloys at temperatures $T = 373$ K and 590 K, respectively. Simulation supercells contained liquid slabs with two free surfaces normal to the z axis. The slabs had dimensions $L_0 L_0 \alpha L_0$, L_0 , and α and were chosen so that the average initial ion number density in the slab coincided with the known bulk ion number density of the system at the temperature [20,21], i.e., $\rho_0(\text{Na}_{0.3}\text{K}_{0.7}) = 0.01487 \text{ \AA}^{-3}$, and $\rho_0(\text{Li}_{0.4}\text{Na}_{0.6}) = 0.02824 \text{ \AA}^{-3}$. For $\text{Na}_{0.3}\text{K}_{0.7}$ the slab contained 2000 ions with $\alpha = 1.73$ leading to a value $L_0 = 42.69 \text{ \AA}$. The slab for the $\text{Li}_{0.4}\text{Na}_{0.6}$ alloy contained 3000 ions with $\alpha = 2.6$ and $L_0 = 34.48 \text{ \AA}$. In both systems, an additional 8 \AA of vacuum were added above and below the slab.

Given the ionic positions at time t , the electron density was expanded in plane waves and the energy functional was minimized with respect to the plane wave coefficients yielding the ground state electronic density, energy, and the forces on the ions via the Feynman-Hellman theorem, and using which the ion positions and velocities were updated. For both systems equilibration lasted for 20 ps. The cutoff energy for the plane wave expansion in the $\text{Na}_{0.3}\text{K}_{0.7}$ ($\text{Li}_{0.4}\text{Na}_{0.6}$) alloy was 5.8 Ry (7.5 Ry), the ion time step was 0.0065 ps (0.0040 ps), and the calculation of properties was made averaging over further 320 ps (220 ps).

During the simulations the slabs contracted and the average total ion densities increased in response to the zero external pressure. In the $\text{Na}_{0.3}\text{K}_{0.7}$ alloy, the total ion

density in the central region of the slab increased by 11% (6% for Na and 5% for K) and the concentration increased to $x_{\text{Na}} = 0.32$ because of the K segregation at the interface. For the $\text{Li}_{0.4}\text{Na}_{0.6}$ alloy, the total ion density in the central region of the slab increased by 15% (7% for Na and 8% for Li) and the concentration increased to $x_{\text{Li}} = 0.41$ due now to the Na segregation.

Figure 1 shows the longitudinal partial [$\rho_{\text{K}}(z)$, $\rho_{\text{Na}}(z)$] and total [$\rho_{\text{NaK}}(z)$] ion density profiles in the $\text{Na}_{0.3}\text{K}_{0.7}$ alloy which have been computed from a histogram of the particle positions relative to the slab's center of mass. $\rho_{\text{NaK}}(z)$ shows a distinct stratification for about four layers into the bulk liquid, which supports the predictions of Tostmann *et al.* [3] from their small wave vector reflectivity measurements. The oscillatory features of $\rho_{\text{NaK}}(z)$ are qualitatively similar to those already observed and/or calculated in several one-component liquid metals [2,7,8] as well as in the Monte Carlo results of Rice *et al.* [5,9] for the $\text{Na}_{0.5}\text{Cs}_{0.5}$, $\text{In}_{0.25}\text{Ga}_{0.75}$, and $\text{Ga}_{0.86}\text{Pb}_{0.14}$ liquid alloys. The

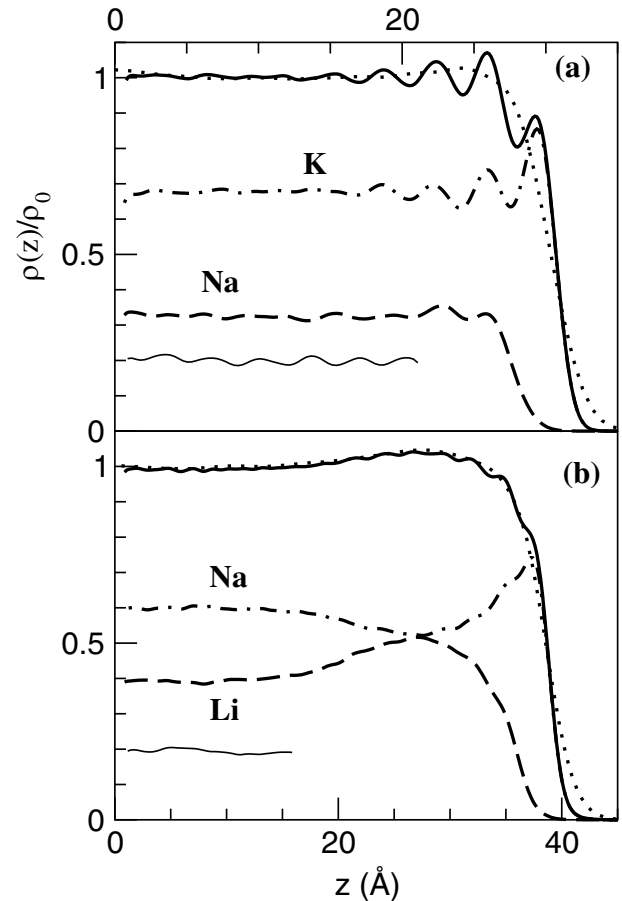


FIG. 1. Valence electron (dotted line), partial (dashed and dash-dotted lines) and total ion (full line) density profiles normal to the liquid-vapor interface in the $\text{Na}_{0.3}\text{K}_{0.7}$ (a) and $\text{Li}_{0.4}\text{Na}_{0.6}$ (b) liquid alloys. The densities are plotted relative to the respective slab's bulk density. The thin continuous horizontal lines at around 0.2 are the x transverse ion density profiles.

oscillations in $\rho_{\text{NaK}}(z)$ have a wavelength of $\approx 3.7 \text{ \AA}$ which suggests a Bragg-like peak in the XR curve at $q \approx 2\pi/3.7 = 1.7 \text{ \AA}^{-1}$, close to the position of the main peak of the measured total static structure factor at $q \approx 1.65 \text{ \AA}^{-1}$ [12]. Qualitatively similar behavior is also seen in the partials $\rho_{\text{K}}(z)$ and $\rho_{\text{Na}}(z)$ which oscillate in phase about their respective bulk values. In contrast, the valence electronic density profile, also shown in Fig. 1, is structureless and decreases monotonically at the liquid-vapor interface.

In order to investigate the outer region of the slab in more detail, we have partitioned the $\rho_{\text{NaK}}(z)$ into slices located between consecutive minima of the oscillations, with the outer slice being $\approx 3 \text{ \AA}$ wide and stretching from the outermost minimum to the inflection point in the decaying total ion density profile. At the outermost slice, the relative change in the total ion number density was $\approx -23\%$, whereas for the next two slices the respective

values were $\approx -4.5\%$ and -1% . These density variations were also matched by changes in the alloy concentration as shown in Figs. 1 and 2. Specifically, K is segregated into the outermost slice which becomes an almost pure K monolayer ($x_{\text{K}} \approx 0.95$). Some expulsion from the surface of the component with the smaller surface tension is anticipated, but this surface segregation of K is much stronger than expected from the $\approx 60\%$ smaller surface tension of K than Na at their melting points. Moreover, the segregation is mainly restricted to the outermost slice as the adjacent slice contains $x_{\text{K}} \approx 0.72$ and other inner slices have the bulk value, $x_{\text{K}} \approx 0.68$, which is attained at about 8.5 \AA from the interface. On the whole, these results follow the trends suggested by Rice and co-workers [5,9] for homovalent binary alloys, with the exception of the deficiency of the segregating component in the second layer.

Qualitatively different results have been obtained for the $\text{Li}_{0.4}\text{Na}_{0.6}$ alloy, whose longitudinal partial $[\rho_{\text{Li}}(z), \rho_{\text{Na}}(z)]$ and total $[\rho_{\text{LiNa}}(z)]$ ion density profiles are also shown in Fig. 1. Now, the total ion profile, $\rho_{\text{LiNa}}(z)$, is rather structureless and as the interface region is approached there are three weak oscillations. These oscillations are real features and not artifacts due to the finite size of the simulation box. This is suggested by the calculated total (x and y) transverse ionic density profiles shown in Fig. 1, which are rather uniform albeit with some noise commensurate with the structure of the $\rho_{\text{LiNa}}(z)$ in the central region of the slab. The oscillations in $\rho_{\text{LiNa}}(z)$ have a wavelength of $\approx 2.9 \text{ \AA}$, implying a Bragg-like peak in the XR curve at $\approx 2\pi/2.9 = 2.15 \text{ \AA}^{-1}$, whereas the position of the main peak in the observed total static structure factor is $q \approx 2.10 \text{ \AA}^{-1}$ [13]. The shape of the total longitudinal ion density profile is determined by the partials, $\rho_{\text{Li}}(z)$ and $\rho_{\text{Na}}(z)$, which differ substantially from those for the $\text{Na}_{0.3}\text{K}_{0.7}$ alloy and, furthermore, show no resemblance to the longitudinal partial density profiles obtained for other liquid binary systems [5,9] where the longitudinal partial profiles always showed oscillations about the respective bulk value. The shape of both $\rho_{\text{Li}}(z)$ and $\rho_{\text{Na}}(z)$ is attributed to the interplay of the expected surface segregation effect and the strong homocoordinating tendencies of this alloy, which favor the surrounding of an ion by others of the same species. The lower surface tension of Na (50% smaller than that of Li, at their respective melting points) induces a Na monolayer at the interface, but now the homocoordinating tendencies lead to further accumulation of Na giving rise to a $\rho_{\text{Na}}(z)$ which from its maximum value near the interface decreases smoothly apart from three very weak oscillations, goes through a minimum, and then approaches its bulk value.

Again, we have divided the outer region of the slab into slices according to the previous scheme in order to investigate the structure in more detail. The outer slice is 2.8 \AA wide and the inner 2.9 \AA wide each. The total ion number density in the outer slices departs significantly from the

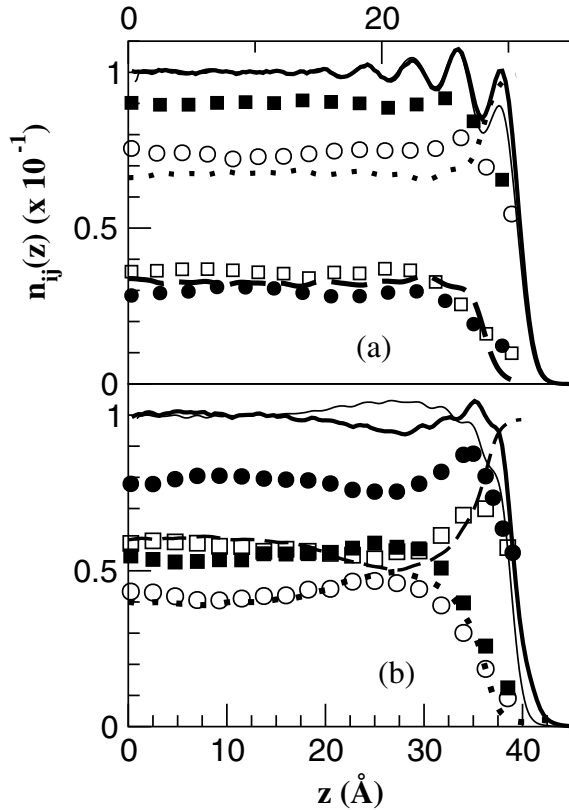


FIG. 2. (a) Calculated z -dependent coordination numbers, $n_{ij}(z)$, for the $\text{Na}_{0.3}\text{K}_{0.7}$ liquid alloy. n_{NaNa} (full circles), n_{NaK} (open circles), n_{KNa} (open squares), and n_{KK} (full squares). The broken (dotted) line is the Na (K) local concentration. (b) The same for the $\text{Li}_{0.4}\text{Na}_{0.6}$ liquid alloy. n_{NaNa} (full circles), n_{NaLi} (open circles), n_{LiNa} (open squares) and n_{LiLi} (full squares). The broken (dotted) line is the Na (Li) local concentration. In both figures the full thick line is the total electron density profile (core + valence) normalized to the slab bulk value, and the thin line is the total ion density profile.

bulk value. For the outermost slice the relative change in the total ion number density was $\approx -36\%$, and for the next two slices the changes were $\approx -19\%$ and -5% . Likewise, the alloy concentration varies substantially with depth, as shown in Figs. 1 and 2. For the outer slice $x_{\text{Na}} \approx 0.99$, whereas for the adjacent inner five slices the concentrations were $x_{\text{Na}} \approx 0.73, 0.59, 0.52, 0.51,$ and 0.53 , and the bulk value, $x_{\text{Na}} = 0.59$, is reached only $\approx 25 \text{ \AA}$ from the interface.

Experimental study of the liquid-vapor interface is usually performed with XR and/or grazing incidence x-ray diffraction, techniques which measure the total electron density distribution. Using the calculated longitudinal ion density profiles we have constructed the total electron (core plus valence) density profiles which are depicted in Fig. 2. For the $\text{Na}_{0.3}\text{K}_{0.7}$ alloy, the total longitudinal electron density profile follows closely the ion profile except for the first oscillation which is enhanced because of the increased relative contribution of the K, with 18 versus 10 core electrons for Na, in the expelled K monolayer. Once again, the most substantial changes occur in the $\text{Li}_{0.4}\text{Na}_{0.6}$ alloy. Over a wide region from the interface to $\approx 25 \text{ \AA}$ into the slab the shape of the total longitudinal electron profile is strongly influenced by the $\rho_{\text{Na}}(z)$ (Na has ten core electrons versus two for Li) and shows appreciable differences in shape from the ion density profile.

In summary, *ab initio* MD simulations of the liquid-vapor interface have been performed for two liquid binary alloys with rather different bulk ordering tendencies. The $\text{Na}_{0.3}\text{K}_{0.7}$ alloy is generally regarded as a nearly ideal mixture and the calculated total longitudinal ion and electron density profiles show layered structures similar to those obtained for the pure alkali metals, although somewhat less marked. In contrast, the $\text{Li}_{0.4}\text{Na}_{0.6}$ liquid alloy has a rather weak layered structure at the interface and the partial density profiles show no resemblance to those for the pure alkali metals, effects which we attribute to the strong homocoordinating tendencies in this bulk alloy. Finally, we note that whereas the partial density profiles in the $\text{Na}_{0.3}\text{K}_{0.7}$ alloy loosely follow the trends proposed by Rice and co-workers for binary homovalent liquid alloys, this pattern does not hold for the $\text{Li}_{0.4}\text{Na}_{0.6}$ alloy, whose behavior, moreover, points to a significant influence of the ordering tendencies on the structure of the liquid-vapor interface.

L. E. G. and D. J. G. acknowledge financial support from the DGES (MAT2002-04393-CO2-01) and the Physics Department at Queen's University. M. J. S. acknowledges the support of the NSERC of Canada.

- [1] J. S. Rowlinson and B. Widom, in *Molecular Theory of Capillarity* (Clarendon, Oxford, 1982); J. Penfold, Rep. Prog. Phys. **64**, 777 (2001).
- [2] O. M. Magnussen *et al.*, Phys. Rev. Lett. **74**, 4444 (1995); M. Regan *et al.*, Phys. Rev. Lett. **75**, 2498 (1995); E. DiMasi *et al.*, Phys. Rev. B **58**, R13419 (1998); **59**, 783 (1999).
- [3] M. J. Regan *et al.*, Phys. Rev. B **55**, 15874 (1997); H. Tostmann *et al.*, Phys. Rev. B **61**, 7284 (2000); E. DiMasi *et al.*, Phys. Rev. Lett. **86**, 1538 (2001); O. Shpyrko *et al.*, Phys. Rev. B **67**, 115405 (2003).
- [4] N. Lei, Z. Huang, and S. A. Rice, J. Chem. Phys. **104**, 4802 (1996); **105**, 9615 (1996).
- [5] N. Lei, Z. Huang, and S. A. Rice, J. Chem. Phys. **107**, 4051 (1997).
- [6] A. Braslau *et al.*, Phys. Rev. Lett. **54**, 114 (1985); B. M. Ocko *et al.*, Phys. Rev. Lett. **72**, 242 (1994); L. B. Lurio *et al.*, Phys. Rev. Lett. **68**, 2628 (1992).
- [7] M. P. D'Evelyn and S. A. Rice, Phys. Rev. Lett. **47**, 1844 (1981); J. Chem. Phys. **78**, 5225 (1983); J. G. Harris, J. Gryko, and S. A. Rice, J. Chem. Phys. **87**, 3069 (1987).
- [8] D. Chekmarev, M. Zhao, and S. A. Rice, J. Chem. Phys. **109**, 768 (1998); **109**, 1959 (1998); Phys. Rev. E **59**, 479 (1999).
- [9] J. Gryko and S. A. Rice, J. Chem. Phys. **80**, 6318 (1984); S. A. Rice and M. Zhao, Phys. Rev. B **57**, 13501 (1998); M. Zhao and S. A. Rice, Phys. Rev. B **63**, 085409 (2001).
- [10] L. E. González *et al.*, J. Phys. Condens. Matter **8**, 4465 (1996).
- [11] D. J. González *et al.*, Phys. Rev. E **69**, 031205 (2004).
- [12] B. P. Alblas and W. van der Lugt, J. Phys. F **10**, 531 (1980); B. P. Alblas *et al.*, Physica (Amsterdam) **101B+C**, 177 (1980).
- [13] H. Ruppertsberg and W. Knoll, Z. Naturforsch. A **32**, 1374 (1977).
- [14] R. R. Hultgren, R. L. Orr, P. D. Anderson, and K. K. Kelly, *Selected Values of Thermodynamic Properties of Metals and Alloys* (Wiley, New York, 1963).
- [15] F. A. Kanda, R. C. Faxon, and D. V. Keller, Phys. Chem. Liq. **1**, 61 (1968); H. K. Schurmann and R. D. Parks, Phys. Rev. Lett. **27**, 1790 (1971); P. D. Feitsma *et al.*, Physica (Amsterdam) **79B+C**, 35 (1975).
- [16] P. Hohenberg and W. Kohn, Phys. Rev. **136**, 864 (1964).
- [17] W. Kohn and L. J. Sham, Phys. Rev. **140**, A1133 (1965).
- [18] D. J. González *et al.*, Phys. Rev. B **65**, 184201 (2002); L. E. González *et al.*, J. Phys. Condens. Matter **13**, 7801 (2001).
- [19] J. Blanco *et al.*, Phys. Rev. E **67**, 041204 (2003).
- [20] M. J. Huijben *et al.*, Scr. Metall. **10**, 571 (1976).
- [21] J. Jost *et al.*, J. Phys. Condens. Matter **6**, 321 (1994).